The Effect of Adding Aluminium on the Performance of ZnO NRs/PANi in Their Application as Photoelectrochemical Water Splitting

Eprilia Trikusuma Sari, Nandang Mufti*, Anissa Chairani Alfin Nadhira, Hari Wisodo, and Markus Diantoro

Department of Physics, Faculty of Mathematics and Natural Sciences, Universitas Negeri Malang, Jl. Semarang 5, Malang, 65145, Indonesia
**Corresponding author:nandang.mufti.fmipa@um.ac.id*

Article history:
Received: 30 October 2023 / Received in revised form: 20 November 2023 / Accepted: 24 November 2023
Available online 27 November 2023

ABSTRACT

Photoelectrochemical (PEC) is a new renewable energy technology that converts H_2O into hydrogen and oxygen gas with the help of sunlight. A photoelectrochemical cell device consists of three main components, one of which is the photoanode. One of the materials that can be used as a photoanode is ZnO which has good electrical properties and is non-toxic. Nanorods-structured ZnO has the advantage of being able to increase light absorption due to its high surface area. However, the resulting performance is still quite low. So it is necessary to make modifications to the photoanode, one of which is by adding aluminium material to ZnO NRs, which has the potential to increase the conductivity of PEC in the production of H_2 and O_2 in H_2O. To overcome the loss of samples during testing, the thin film will be coated with conductive polymers such as polyaniline (PANi), which has high conductivity, can increase photoactive ability, and has good corrosion resistance. In this study, the performance of ZnO NRs/PANi against AZO NRs/PANi will be studied by adding aluminium. The ZnO nanorods were synthesized by Hydrothermal method, Aluminium was deposited on ZnO NRs by DC Magnetron Sputtering method, and PANi was synthesized by polymerization method. From the XRD characterization results, it can be concluded that the addition of aluminium to ZnO NRs/PANi causes an increase in crystallinity and peak shift. SEM characterization shows that the addition of Al to ZnO NRs/PANi causes the porosity value to increase. In addition, UV-Vis characterization showed that the addition of Al material to the ZnO NRs/PANi thin film resulted in a wider range of absorbance of the light spectrum. Then, Cyclic Voltammetry test shows that the addition of aluminium increases the efficiency of the photoelectrochemical.

Keywords: *AZO NRs, PANi, photoelectrochemical, water splitting.*

I. Introduction

Photoelectrochemical (PEC) is a technology that converts light energy into electrical energy through electrolysis [1]–[3]. Photoelectrochemical technology has a significant impact because utilizing this technology can produce clean and sustainable electrical energy [4]. So that development of photoelectrochemical technology can also reduce the cost of energy production to be more affordable [5]. One of the most important constituent components that plays a role in converting photons into electron-hole pairs, namely the photoanode [6]. Semiconductor materials commonly used as photoanode constituents include TiO_2, ZnO, WO_3, and CuO [7]. Among these materials, ZnO has the potential as an anode constituent material because of its advantages of having good electrical properties, non-toxicity, easy fabrication, and large binding energy of 60 meV [8]–[10]. ZnO nanostructures such as ZnO nanorods were chosen because they have high electron mobility

DOI: 10.17977/um016v7i22023p202

[11], an energy band gap of ~3.37 eV [8], good photocatalyst activity, and structural stability [12]. ZnO nanorods-based PEC research conducted by Tan et al., produced a current density of up to 0.483 mA/cm^2 [13].

Research on ZnO NRs/Au-based PEC technology produced a current density of 30 µA/cm^2 [14]. Other research on ZnO/Fe_3O_4 still produces a fairly low current density of 70 µA/cm^2 [15]. However, the resulting performance is still quite low. Therefore, to obtain high performance and highly to splitting of H_2O into H_2 and O_2, the addition of metal materials with elements such as Al, N, Mg, and Cd [16]. So in this study, modifications were made to the photoanode by adding aluminium material to ZnO NRs which has the potential to increase the conductivity of PEC in the production of H_2 and O_2 in H_2O. Among other metal materials, Aluminium (Al) has a very high potential to be developed because of its high stability and is able to reduce the resistivity of ZnO [17]. Research by Shet et al. on Photoelectrochemical based ZnO NRs/Al (AZO NRs) with RF Magnetron Sputtering method at 300 W power variation produces the highest current density, namely 0.36 mA/cm^2 [18]. Another study by Zong et al. on solar cells based on ZnO NRs/Al, SiO_2 with the Co-Sputtering method at a power variation of 25 W obtained the highest current density results of 0.37 mA/cm^2 [19]. Recent research conducted by Rabell et al. regarding Photoelectrochemical proved that increasing the addition of Al to ZnO (AZO) made the photocatalytic activity for producing hydrogen gas higher [16].

However, so far during the photoelectrochemical performance testing process, sample loss often occurs. Sample loss during the testing process can affect the stability and lifetime of the photoanode. So, this can be overcome by adding conductive polymers to the ZnO NRs and AZO NRs photoanode. A conductive polymer is a type of polymer that has electronic and optical properties like metals and mechanical properties like polymers. One of the reasons for using conductive polymers in PEC cells is that they can increase the photoactive ability, efficiency, and corrosion resistance of the sample [20], [21]. PANi is a polymer with high conductivity [22] and has good environmental stability [23]. Research related to conductive polymers in PEC cells has been carried out. It was reported that ZnO/PANi increased the breakdown of H_2O into H_2 and O_2 in wastewater [24]. Polyaniline was reported to increase the photosensitivity of PEC to visible light [23]. Therefore, a study will be carried out on the addition of aluminium to ZnO NRs/PANi as a fuel cell photoanode which is expected to produce high performance.

II. Material and Methods

1. Materials

The primary material in this study used Zinc Acetate Dihydrate powder obtained through Sigma Aldrich (USA). Zinc Nitrate Tetrahydrate powder obtained through kGaA (Germany). Monoethanolamine (MEA), Hexamethylenetetramine (HMTA), Aluminium sputtering target, Aniline, HCl, and Ammonium Peroxidisulfate obtained through Sigma Aldrich (USA). Deionized water obtained through PT. Jayamas Medica Industri (Indonesia).

2. Synthesis of Photoanode

In this research, there are several steps involved. The ZnO nanorods were synthesized in two steps by coating ZnO seed layer on ITO glass using spin-coating method and growing ZnO nanorods by hydrothermal method. Zinc Acetate Dihydrate powder (0.88 g) was dissolved with 20 mL of ethanol p.a. Stirred for 30 minutes with a solution temperature of 70°C. Then add Monoethanolamine (MEA) 0.24 µL and strirer for 1 hour. Deposition on ITO Glass by Spin coating method, then annealing the film at 400°C for 2 hours. The

precursors used to grow ZnO nanorods were synthesized from Zinc Nitrate Tetrahydrate (0.58 g) and HMTA (0.32 g) were dissolved with 50 mL DI water. After that, stir the solution for 45 minutes at room temperature. The ZnO seed layer film was immersed in the precursor solution for 5 hours at 155°C. Then annealing it films for 2 hours at 550°C. Furthermore, additional material aluminium (Al) was coated by DC Magnetron Sputtering method. Aluminium metal material was deposited on ZnO NRs by DC Magnetron Sputtering method. Aluminium sputtering was carried out for 15 minutes with 80 W power. After that, the sample was annealed at 150°C for 30 minutes. In addition, to synthesize PANI it is done by dissolving 1.82 mL Aniline in 0.603 mL of HCl (1 M). At the same time 5.71 grams of Ammonium Peroxidisulfate [$(NH)_4S_2O_8$] was dissolved in 50 mL of distilled water. Both solutions were allowed to stand for 1 hour. Then the two solutions were mixed and stirred at 600 rpm for 1 hour. Then allowed to stand for 24 hours until a precipitate formed. Then washed until pH 7. Finally dried in oven at 100 ºC for 40 minutes. To coat the PANi polymer, the spin coating method was carried out at a speed of 3000 rpm for 1 minute. Then ZnO NRs/PANi and AZO NRs/PANi film as photoanodes was annealed at 100°C for 1 hour.

3. Cyclic Voltammetry Testing

The ability of the sample was tested using Cyclic Voltammetry (CV) testing scheme of three electrodes in bright conditions with a power of 100 mW on a sample with an active area of 1 cm^2. The electrolyte used was 0.1 M Na_2SO_4. In the test, the sample (ZnO NRs/PANi & AZO NRs/PANi) acts as working electrode, platinum electrode as counter electrode, and Ag/AgCl as reference electrode. CV testing was carried out with scan rates of 50 and 100 mV/s.

4. Characterization

There were several characterizations performed in this study, including XRD, SEM, and UV-Vis. X-ray Diffraction (XRD) analysis was performed using PanAnalytical Expert Pro with a diffraction angle of $20 - 80°$. Then, Scanning Electron Microscope (SEM) analysis was carried out to analyse the morphology of the sample both from its surface structure with a magnification of 50,000 times and from a cross-section with a magnification of 100,000 times. SEM analysis was carried out using FEI type INSPECT-S50. Furthermore, UV-Vis Spectrophotometer analysis was carried out to determine the absorbance and band gap of the material. UV-Vis analysis was carried out at a wavelength of 200-800 nm using Analytic Jena Specord 200 plus.

III. Results and Discussions

It is known that ZnO nanorods (ZnO NRs) have hexagonal-Wurtzite crystal structure with space group P6(3)mc. Furthermore, Figure 1 shown the diffraction pattern of ZnO NRs/PANi and AZO NRs/PANi thin film. In Figure 1, the diffraction pattern of ZnO peaks was detected at angles 31.57º (100), 34.36º (002), 36.18º (101), 47.56º (102), 56.58º (110), 62.82º (103), and 67.95º (201). The appearance of the hkl (002) plane diffraction peak concluded that the nanorods formed have a hexagonal wurtzite structure and are oriented towards the c-axis. Then Figure 2 shows the peak shift diffraction pattern of ZnO NRs/PANi and AZO NRs/PANi.

Figure 2 shows the 2θ positions of the three main peaks of the ZnO NRs/PANi and AZO NRs/PANi film diffraction pattern in the hkl (100), (002), and (101) planes. It is shown in Table 1 that there has been a shift in the positions of the three peaks. This shift is known to

occur due to shrinkage of the ZnO nanorods lattice. This is because the Zn^{2+} atom which has a radius of 0.74 Å, is replaced by an Al^{3+} atom which has a radius of only 0.53Å [25].

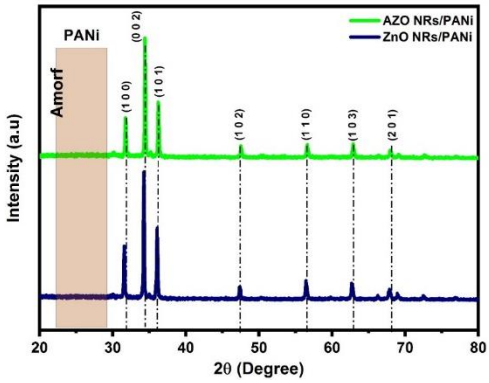

Fig. 1. Diffraction pattern of ZnO NRs/PANi and AZO NRs/PANi

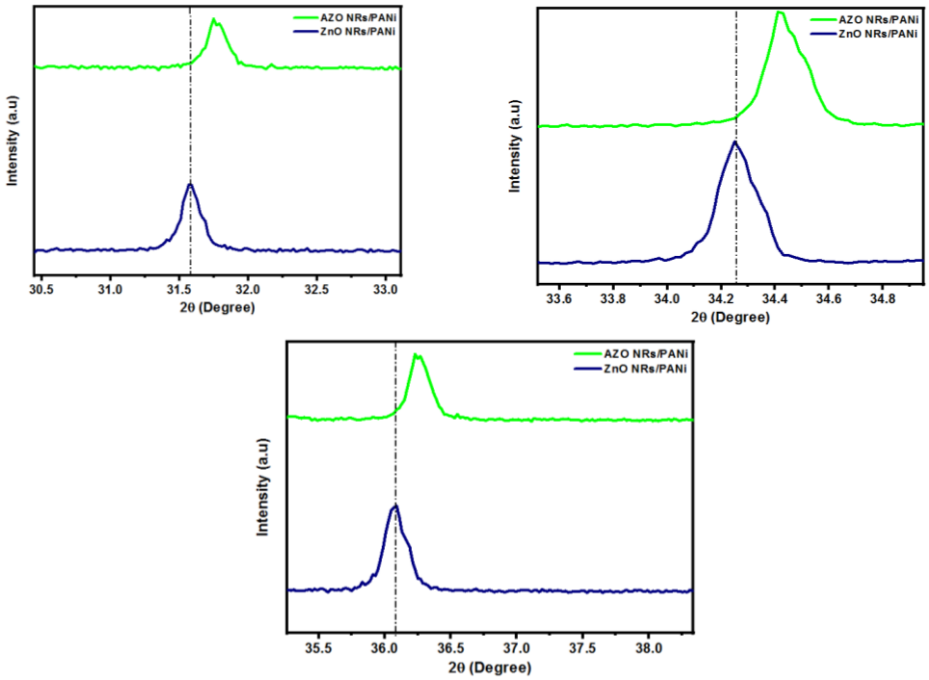

Fig. 2. Peak shift diffraction pattern of ZnO NRs/PANi and AZO NRs/PANi

Table 1. Diffraction angle shift of the first three peaks of thin film

Sampel	Hkl		
	(1 0 0)	(0 0 2)	(1 0 1)
ZnO NRs/PANi	31.57°	34.36°	36.18°
AZO NRs/PANi	31.63°	34.39°	36.23°

The morphology of the samples can be identified from the Scanning Electron Microscopy (SEM) characterization results. Figure 3 shows the surface morphology of ZnO nanorods (ZnO NRs) and AZO nanorods (AZO NRs) shown from SEM results with a magnification of 50,000 times. Based on the SEM results as shown in Figure 3 (a), ZnO NRs

have a hexagonal wurtzite structure with a fairly even distribution and have a growth direction perpendicular to the ITO substrate surface. This is in accordance with research conducted by Abadi et al [15]. The addition of Aluminium material on ZnO NRs results in surface morphology that tends to be rough. The rough surface of AZO NRs is caused by the merging of grain boundaries between ZnO and Al [26].

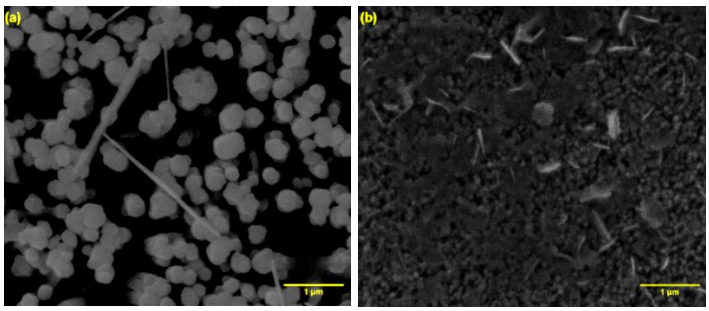

Fig. 3. Surface morphology of (a) ZnO Nanorods and (b) AZO Nanorods

Furthermore, Figure 4 shows the SEM cross section results of ZnO NRs/PANi and AZO NRs/PANi thin films. Cross section results can show the thickness of ZnO NRs/PANi and AZO NRs/PANi thin films. The addition of Aluminium material on ZnO NRs causes the thickness of the thin film to increase. The same results have also been reported by Rosli et al. [27].

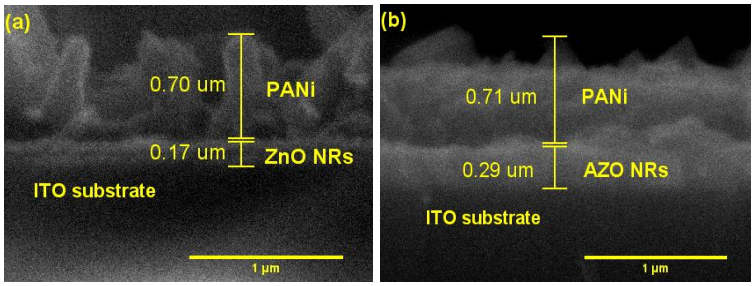

Fig. 4. Cross section of thin films of (a) ZnO NRs/PANi and (b) AZO NRs/PANi

In addition, the SEM characterization results can also be used to determine the porosity value as seen from the surface morphology of the material. Figure 5 is a three-dimensional graph of the porosity distribution of ZnO NRs/PANi and AZO NRs/PANi thin films.

The porosity value is the ratio between the empty volume and the total volume of the entire sample. The higher porosity value indicates that the greater the volume of space not occupied by AZO NRs/PANi [28]. Based on the calculation of the porosity value, it is found that the addition of Al material to ZnO NRs/PANi can increase the porosity of the thin film. This is also in accordance with research conducted by Hong et al, where an increase in porosity occurs because aluminium can inhibit the growth of ZnO grains [29]. In addition, the high porosity value also indicates that the active surface area produced is larger, so as to improve the performance of the photoanode in photoelectrochemical [30]. The results of porosity values are presented in Table 2.

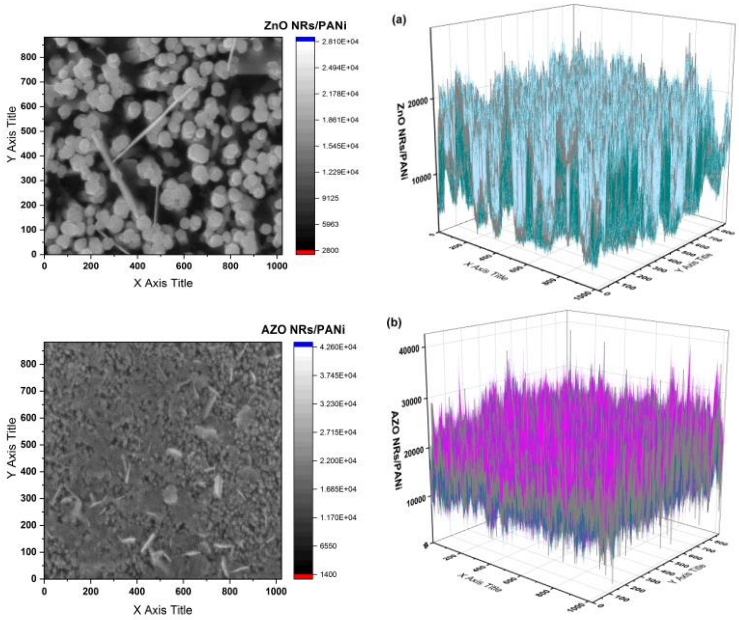

Fig. 5. Porosity graphs of (a) ZnO NRs/PANi and (b) AZO NRs/PANi

Table 2. Porosity of ZnO NRs/PANi and AZO NRs/PANi Thin Films

Sample	Porosity (%)
ZnO NRs/PANi	60.76
AZO NRs/PANi	61.58

Optical properties including absorbance and band gap of the thin films were obtained from Ultra-Violet Visible Spectrophotometry (UV-Vis) characterization. Figure 6 shows the absorbance graph of ZnO NRs, PANi, ZnO NRs/PANi, and AZO NRs/PANi thin films.

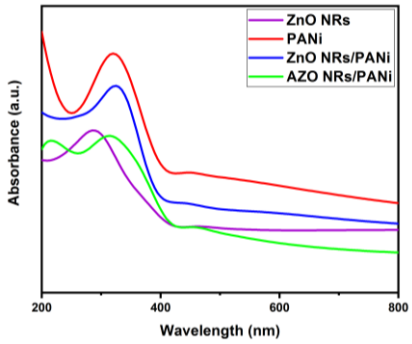

Fig. 6. Absorbance graphs of ZnO NRs, PANi, ZnO NRs/PANi, and AZO NRs/PANi

Figure 6 shows the average absorbance edge of the thin film is in the wavelength range of 286-324 nm. This shows that the AZO NRs/PANi thin film is only able to absorb ultraviolet light. The same results have also been reported by research conducted by Cesar et al [31]. Based on Figure 6, it can be seen that the addition of Al material to the ZnO NRs/PANi thin film results in a wider range of absorption (absorbance) of the light spectrum. This can cause more light absorption so as to improve the performance of AZO NRs/PANi photoanodes in photoelectrochemical cell [32].

Furthermore, to determine the band gap value of material, the optical band gap calculation is carried out using the Tauc plot method. The following is the Tauc plot equation (1) [33]:

$$(\alpha hv)^2 = A(hv - E_g) \quad \text{(1)}$$

The value of α is the absorption coefficient of the material, *h* is the Planck constant, *v* is the frequency of the incident photon, while *A* is the energy constant, and E_g is the band gap energy value. The results of the band gap energy calculation of the film base materials, ZnO NRs and PANi, are shown in Figures 7(a) and 7(b). In addition, the calculation of the band gap energy value is also carried out to determine the difference when ZnO NRs/PANi is added with Aluminium. From the Tauc Plot fitting results, it can be seen that the addition of Al material to ZnO NRs/PANi results in an increase in band gap energy [33]. Furthermore, the fitting results of ZnO NRs/PANi and AZO NRs/PANi thin films are shown in Figures 7(c) and 7(d).

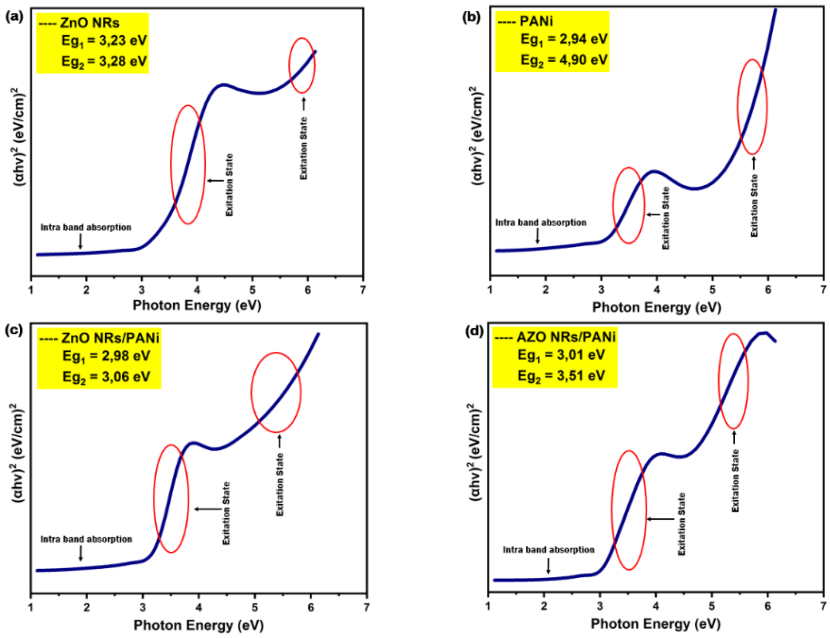

Fig. 7. Bandgap fittings of (a) ZnO NRs, (b) PANi, (c) ZnO NRs/PANi, and (d) AZO NRs/PANi

Table 3 shows the absorbance results along with the band gap energy values obtained by the samples.

Table 3. Absorbance value and band gap energy of ZnO NRs/PANi & AZO NRs/PANi Thin Films

Sample	Absorbance (nm)	Band gap Energy (eV)	
		Eg_1	Eg_2
ZnO NRs/PANi	324	2.98	3.06
AZO NRs/PANi	316	3.01	3.51

Based on the results of the data analysis presented in Table 3, it shows that the absorbance value of light is inversely proportional to the band gap energy value obtained. The AZO NRs/PANi thin film experiences a blue shift in its band gap when compared to

ZnO NRs/PANi [34]. In general, the band gap in semiconductors is affected by the Burstein-Moss effect, compressive strain, and Urbach tail shift [35], [36]. The increase in the band gap of ZnO NRs when added with aluminium (Al) is due to the reduction in pressure [37]. This band gap increase is also influenced by the Burstein-Moss effect where aluminium shifts the Fermi level to the conduction band [38].

Based on the CV test results, a graph between current density and bias voltage was obtained, as shown in Figure 8.

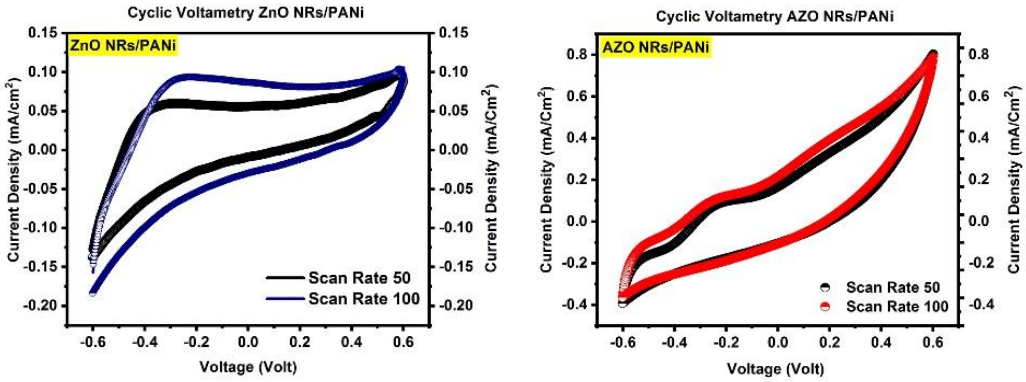

Fig. 8. Cyclic voltametry curve of ZnO NRs/PANi and AZO NRs/PANi

From Figure 8, it is known that the addition of Al material to ZnO NRs results in a higher current density. It is also proportional to the efficiency or performance of the photoelectrochemical cell. In the three-electrode testing scheme, the efficiency value can be calculated using Equation (2) [39]:

$$\eta(V_{app}) = \frac{I(V_{app})\times\Delta G\times\varepsilon}{I(V_{app})\times V+P\times A} \quad \text{.....(2)}$$

Where, $\eta(V_{app})$ is the efficiency calculated when using the bias voltage. $I(V_{app})$ is the current produced. ΔG adalah Gibbs free energy based on the breakdown of water molecules is 1.23 V. V is the max voltage applied, ε is the Faraday efficiency which is 100%. P is the beam power used per unit area and A is the active area of the sample [39].

Table 4. Current density and efficiency performance of CV test results

Sample	Current Density (mA/cm^2)	Efficiency (%)
ZnO NRs/PANi	0.1	0.123
AZO NRs/PANi	0.8	0.979

The photoelectrochemical water splitting performance results obtained are higher than the PEC research conducted by Abadi et al. with ZnO NRs/Au/PANi photoanodes which produced a current density of 10.6 μA/cm^2 with a performance of 0.16% [40]. This research has also been proven by Rabell et al. where the addition of aluminium to ZnO as a photoelectrochemical is able to increase the breakdown of H_2O into H_2 and O_2 higher [16]. So it can be concluded that the addition of aluminium to ZnO is considered capable of improving the performance of photoelectrochemical cells, as evidenced by the increase in the efficiency value of the photoelectrochemical cell. In addition, the addition of PANi

conductive polymer is also able to increase the current density value and prevent loss during the testing process so that it has good stability and lifetime.

IV. Conclusions

The addition of aluminium to ZnO NRs/PANi causes an increase in crystallinity and a peak shift. The results from SEM also show that the addition of Al to ZnO NRs/PANi causes the thickness of the thin film to increase and increases the porosity value. Apart from that, the UV-Vis characterization shows that the absorbance decreases, but the addition of Al material to the ZnO NRs/PANi thin film results in a wider range of absorption (absorbance) of the light spectrum. This result shows that the sample is only able to absorb UV light. For the ZnO NRs/PANi band gap, when aluminium is added, it increases. This increase in band gap energy may be attributed to the Burstein-Moss effect where Aluminium shifts theFermi level to the conduction band. Then, from Cyclic Voltammetry results obtained, it shows that the addition of aluminium material to the ZnO NRs/PANi thin film can produce a photoelectrochemical cell photoanode with better performance for application as a fuel cell in PEC Water Splitting technology.

Acknowledgment

The authors would like to appreciate Universitas Negeri Malang, which provides the facilities to conduct the research and DRTPM through the research grant scheme PTM with contract number of 20.6.76/UN32.20.1/LT/2023.

References

[1] C. Acar and I. Dincer, "Energy and exergy analyses of a novel photoelectrochemical hydrogen production system," *Int. J. Hydrog. Energy*, vol. 42, no. 52, pp. 30550–30558, Dec. 2017, doi: 10.1016/j.ijhydene.2017.10.008.

[2] A. Grimm, W. A. de Jong, and G. J. Kramer, "Renewable hydrogen production: A techno-economic comparison of photoelectrochemical cells and photovoltaic-electrolysis," *Int. J. Hydrog. Energy*, vol. 45, no. 43, pp. 22545–22555, Sep. 2020, doi: 10.1016/j.ijhydene.2020.06.092.

[3] W. Yang, R. R. Prabhakar, J. Tan, S. D. Tilley, and J. Moon, "Strategies for enhancing the photocurrent, photovoltage, and stability of photoelectrodes for photoelectrochemical water splitting," *Chem. Soc. Rev.*, vol. 48, no. 19, pp. 4979–5015, Sep. 2019, doi: 10.1039/C8CS00997J.

[4] A. Thakur, D. Ghosh, P. Devi, K.-H. Kim, and P. Kumar, "Current progress and challenges in photoelectrode materials for the production of hydrogen," *Chem. Eng. J.*, vol. 397, p. 125415, Oct. 2020, doi: 10.1016/j.cej.2020.125415.

[5] S. F. Ahmed, M. Mofijur, S. Nuzhat, N. Rafa, and A. Musharrat, "Sustainable hydrogen production: Technological advancements and economic analysis," *Int. J. Hydrog. Energy*, vol. 47, no. 88, pp. 37227–37255, Oct. 2022, doi: 10.1016/j.ijhydene.2021.12.029.

[6] J. Hu, S. Zhao, X. Zhao, and Z. Chen, "Strategies of Anode Materials Design towards Improved Photoelectrochemical Water Splitting Efficiency," *Coatings*, vol. 9, no. 5, Art. no. 5, May 2019, doi: 10.3390/coatings9050309.

[7] T. A. Dontsova, S. V. Nahirniak, and I. M. Astrelin, "Metaloxide Nanomaterials and Nanocomposites of Ecological Purpose," *J. Nanomater.*, vol. 2019, p. e5942194, Apr. 2019, doi: 10.1155/2019/5942194.

[8] M. A. Borysiewicz, "ZnO as a Functional Material, a Review," *Crystals*, vol. 9, no. 10, Art. no. 10, Oct. 2019, doi: 10.3390/cryst9100505.
[9] M. Sufyan, U. Mehmood, Y. Qayyum Gill, R. Nazar, and A. Ul Haq Khan, "Hydrothermally synthesize zinc oxide (ZnO) nanorods as an effective photoanode material for third-generation Dye-sensitized solar cells (DSSCs)," *Mater. Lett.*, vol. 297, p. 130017, Aug. 2021, doi: 10.1016/j.matlet.2021.130017.
[10] M. Singh, D. Vadher, V. Dixit, and C. Jariwala, "Synthesis, optimization and characterization of zinc oxide nanoparticles prepared by sol–gel technique," *Mater. Today Proc.*, vol. 48, pp. 690–692, 2022, doi: 10.1016/j.matpr.2021.08.145.
[11] N. Mufti, M. Tommy Hasan Abadi, A. Yasrina, Sunaryono, and Yudyanto, "Photoelectrochemical Performance of ZnO Nanorods Grown on Stainless Steel Substrate," *IOP Conf. Ser. Mater. Sci. Eng.*, vol. 515, p. 012023, Apr. 2019, doi: 10.1088/1757-899X/515/1/012023.
[12] C. Chen, H. Bai, Z. Da, M. Li, X. Yan, and J. Jiang, "Hydrothermal synthesis of Fe2O3/ZnO heterojunction photoanode for photoelectrochemical water splitting," *Funct. Mater. Lett.*, vol. 08, no. 05, p. 1550058, Oct. 2015, doi: 10.1142/S1793604715500587.
[13] H. J. Tan, Z. Zainal, Z. A. Talib, H. N. Lim, and S. Shafie, "Synthesis of high quality hydrothermally grown ZnO nanorods for photoelectrochemical cell electrode," *Ceram. Int.*, vol. 47, no. 10, pp. 14194–14207, May 2021, doi: 10.1016/j.ceramint.2021.02.005.
[14] W. Zhang, W. Wang, H. Shi, Y. Liang, J. Fu, and M. Zhu, "Surface plasmon-driven photoelectrochemical water splitting of aligned ZnO nanorod arrays decorated with loading-controllable Au nanoparticles," *Sol. Energy Mater. Sol. Cells*, vol. 180, pp. 25–33, Jun. 2018, doi: 10.1016/j.solmat.2018.02.020.
[15] M. T. H. Abadi, E. K. Maula, Sunaryono, S. Zulaikah, H. Setiyanto, and N. Mufti, "Fe3O4/ZnO bilayer for photoelectrochemical properties enhancement of current efficiency," *AIP Conf. Proc.*, vol. 2251, no. 1, p. 040019, Aug. 2020, doi: 10.1063/5.0015839.
[16] G. O. Rabell, M. R. Alfaro Cruz, and I. Juárez-Ramírez, "Photoelectrochemical (PEC) analysis of ZnO/Al photoelectrodes and its photocatalytic activity for hydrogen production," *Int. J. Hydrog. Energy*, vol. 47, no. 12, pp. 7770–7782, Feb. 2022, doi: 10.1016/j.ijhydene.2021.12.107.
[17] H. Aydın, F. Yakuphanoglu, and C. Aydın, "Al-doped ZnO as a multifunctional nanomaterial: Structural, morphological, optical and low-temperature gas sensing properties," *J. Alloys Compd.*, vol. 773, pp. 802–811, Jan. 2019, doi: 10.1016/j.jallcom.2018.09.327.
[18] S. Shet, K.-S. Ahn, T. Deutsch, H. Wang, N. Ravindra, and Y. Yan, "Synthesis and characterization of band gap-reduced ZnO:N and ZnO:(Al,N) films for photoelectrochemical water splitting," *J. Mater. Res.*, vol. 25, no. 1, pp. 69–75, Jan. 2010, doi: 10.1557/JMR.2010.0017.
[19] S. Zhong, M. Morales-Masis, M. Mews, L. Korte, Q. Jeangros, and W. Wu, "Exploring co-sputtering of ZnO:Al and SiO2 for efficient electron-selective contacts on silicon solar cells," *Sol. Energy Mater. Sol. Cells*, vol. 194, pp. 67–73, Jun. 2019, doi: 10.1016/j.solmat.2019.02.005.
[20] G. De Alvarenga, B. M. Hryniewicz, I. Jasper, R. J. Silva, V. Klobukoski, and F. S. Costa, "Recent trends of micro and nanostructured conducting polymers in health and environmental applications," *J. Electroanal. Chem.*, vol. 879, p. 114754, Dec. 2020, doi: 10.1016/j.jelechem.2020.114754.

[21] R. M. Abdelfattah, M. Shaban, F. Mohamed, A. A. M. El-Reedy, and H. M. Abd El-Salam, "A new Synthetic Polymers Based on Polyaniline for Dual-Functional Applications: Photoelectrochemical Water Splitting and Antibacterial Activities," *ACS Omega*, vol. 6, no. 32, pp. 20779–20789, Aug. 2021, doi: 10.1021/acsomega.1c01802.
[22] M. Kandasamy, A. Seetharaman, B. Chakraborty, I. Manohara Babu, J. J. William, and G. Muralidharan, "Experimental and Theoretical Investigation of the Energy-Storage Behavior of a Polyaniline-Linked Reduced-Graphene-Oxide– Sn O 2 Ternary Nanohybrid Electrode," *Phys. Rev. Appl.*, vol. 14, no. 2, p. 024067, Aug. 2020, doi: 10.1103/PhysRevApplied.14.024067.
[23] S. Sharma, S. Singh, and N. Khare, "Enhanced photosensitization of zinc oxide nanorods using polyaniline for efficient photocatalytic and photoelectrochemical water splitting," *Int. J. Hydrog. Energy*, vol. 41, no. 46, pp. 21088–21098, Dec. 2016, doi: 10.1016/j.ijhydene.2016.08.131.
[24] T. Zou, C. Wang, R. Tan, W. Song, and Y. Cheng, "Preparation of pompon-like ZnO-PANI heterostructure and its applications for the treatment of typical water pollutants under visible light," *J. Hazard. Mater.*, vol. 338, pp. 276–286, Sep. 2017, doi: 10.1016/j.jhazmat.2017.05.042.
[25] F. Mouzaia, D. Djouadi, A. Chelouche, L. Hammiche, and T. Touam, "Particularities of pure and Al-doped ZnO nanostructures aerogels elaborated in supercritical isopropanol," *Arab J. Basic Appl. Sci.*, vol. 27, no. 1, pp. 423–430, Jan. 2020, doi: 10.1080/25765299.2020.1833484.
[26] D. Zhang, W. Yu, L. Zhang, and X. Hao, "Progress in the Synthesis and Application of Transparent Conducting Film of AZO (ZnO:Al)," *Materials*, vol. 16, no. 16, Art. no. 16, Jan. 2023, doi: 10.3390/ma16165537.
[27] A. B. Rosli, S. S. Shariffudin, Z. Awang, and S. H. Herman, "AZO nanorods thin films by sputtering method," presented at the 8th International Conference on Nanoscience And Nanotechnology 2017 (Nano-Scitech 2017), Selangor, Malaysia, 2018, p. 020003. doi: 10.1063/1.5036849.
[28] A. Yildiz, H. Cansizoglu, M. Turkoz, R. Abdulrahman, A. Al-Hilo, and T. Karabacak, "Glancing angle deposited Al-doped ZnO nanostructures with different structural and optical properties," *Thin Solid Films*, vol. 589, pp. 764–769, Aug. 2015, doi: 10.1016/j.tsf.2015.06.058.
[29] M.-H. Hong, S.-Y. Jung, T.-J. Ha, W.-S. Seo, Y. S. Lim, and S. Shin, "Thermoelectric properties of mesoporous TiO 2 thin films through annealing temperature and ratio of surfactant," *Surf. Coat. Technol.*, vol. 231, pp. 370–373, Sep. 2013, doi: 10.1016/j.surfcoat.2012.07.035.
[30] X. Sun, W. Luo, L. Chen, L. Zheng, C. Bao, and P. Sun, "Synthesis of porous Al doped ZnO nanosheets with high adsorption and photodecolorizative activity and the key role of Al doping for methyl orange removal," *RSC Adv.*, vol. 6, no. 3, pp. 2241–2251, 2016, doi: 10.1039/C5RA21954J.
[31] D. Q. J. C. Augusto, D. A. F. J. Batista, D. M. N. J. Quinzinho, I. O. Nascimento, D. S. I. Alves, and D. O. Q. M. Gerlania, "Structural and optical properties of Al-doped ZnO thin films produced by magnetron sputtering," *Process. Appl. Ceram.*, vol. 14, no. 2, pp. 119–127, 2020.
[32] X. Chong, L. Li, X. Yan, D. Hu, H. Li, and Y. Wang, "Synthesis, characterization and room temperature photoluminescence properties of Al doped ZnO nanorods," *Phys. E Low-Dimens. Syst. Nanostructures*, vol. 44, no. 7–8, pp. 1399–1405, Apr. 2012, doi: 10.1016/j.physe.2012.03.001.

[33] A. Henni, A. Merrouche, L. Telli, and A. Karar, "Studies on the structural, morphological, optical and electrical properties of Al-doped ZnO nanorods prepared by electrochemical deposition," *J. Electroanal. Chem.*, vol. 763, pp. 149–154, Feb. 2016, doi: 10.1016/j.jelechem.2015.12.037.

[34] S. Kim, S. Lee, J. Kim, J. Kim, D. Y. Kim, and S.-O. Kim, "Effects of Doping with Al, Ga, and In on Structural and Optical Properties of ZnO Nanorods Grown by Hydrothermal Method," *Electron. Mater. Lett.*, vol. 9, Jul. 2013, doi: 10.1007/s13391-013-0048-7.

[35] T. P. Rao, M. C. S. Kumar, S. A. Angayarkanni, and M. Ashok, "Effect of stress on optical band gap of ZnO thin films with substrate temperature by spray pyrolysis," *J. Alloys Compd.*, vol. 485, no. 1–2, pp. 413–417, Oct. 2009, doi: 10.1016/j.jallcom.2009.05.116.

[36] C. Abed, C. Bouzidi, H. Elhouichet, B. Gelloz, and M. Ferid, "Mg doping induced high structural quality of sol–gel ZnO nanocrystals: Application in photocatalysis," *Appl. Surf. Sci.*, vol. 349, pp. 855–863, Sep. 2015, doi: 10.1016/j.apsusc.2015.05.078.

[37] K. Gherab, Y. Al-Douri, C. H. Voon, U. Hashim, M. Ameri, and A. Bouhemadou, "Aluminium nanoparticles size effect on the optical and structural properties of ZnO nanostructures synthesized by spin-coating technique," *Results Phys.*, vol. 7, pp. 1190–1197, 2017, doi: 10.1016/j.rinp.2017.03.013.

[38] J. Jia, A. Takasaki, N. Oka, and Y. Shigesato, "Experimental observation on the Fermi level shift in polycrystalline Al-doped ZnO films," *J. Appl. Phys.*, vol. 112, no. 1, p. 013718, Jul. 2012, doi: 10.1063/1.4733969.

[39] R. H. Coridan, A. C. Nielander, S. A. Francis, M. T. McDowell, V. Dix, and S. M. Chatman, "Methods for comparing the performance of energy-conversion systems for use in solar fuels and solar electricity generation," *Energy Environ. Sci.*, vol. 8, no. 10, pp. 2886–2901, 2015, doi: 10.1039/C5EE00777A.

[40] M. T. H. Abadi, N. A. Sofa, S. Zulaikah, and N. Mufti, "Influence of Au Sputtered in ZnO/Au/PANI Heterostructures Film for Photoelectrochemical Cells," *Mater. Sci. Forum*, vol. 1028, pp. 117–126, 2021, doi: 10.4028/www.scientific.net/MSF.1028.117.